Aeroelastic Flutter of Subsonic Aircraft Wing Section with Control Surface

Dr. Hatem Rahim Wasmi
Assistant Professor
College of Engineering - University of Baghdad
E-mail : hatemrwa@coeng.uobaghdad.edu.iq

Dr. Ali Abdul Mohsin Hasan
Assistant Professor
College of Engineering - University of University
E-mail dralicit@coeng.uobaghdad.edu.iq

Waleed Jasim Mhaimeed
Assistant Lecture
Al-Khwarizmi College of Engineering- University of Baghdad
E-mail waleed_jmm@kecbu.uobaghdad.edu.iq

ABSTRACT

Aeroelastic flutter in aircraft mechanisms is unavoidable, essentially in the wing and control surface. In this work a three degree-of-freedom aeroelastic wing section with trailing edge flap is modeled numerically and theoretically. FLUENT code based on the steady finite volume is used for the prediction of the steady aerodynamic characteristics (lift, drag, pitching moment, velocity, and pressure distribution) as well as the Duhamel formulation is used to model the aerodynamic loads theoretically. The system response (pitch, flap pitch and plunge) was determined by integration the governing equations using MATLAB with a standard Runge–Kutta algorithm in conjunction with Henon's method. The results are compared with previous experimental data. The results show that the aerodynamic loads and wing-flap system response are increased when increasing the flow speed. On the other hand the aeroelastic response led up to limit cycle oscillation when the flow equals or more than flutter speed.

Key word: aeroelastic, wing, control surface, aerodynamic

المرونة الهوائية لرفرفة مقطع جناح طائرة مع اسطح السيطرة في سرعة دون سرعة الصوت

د. حاتم رحيم وسمي
استاذ مساعد
كلية الهندسة-جامعة بغداد

د. علي عبدالمحسن حسن
استاذ مساعد
كلية الهندسة-جامعة بغداد

وليد جاسم محيميد
مدرس مساعد
كلية الهندسة الخوارزمي-جامعة بغداد

الخلاصة

الرفرفة في نظام المائع-هيكل لا يمكن تجنبها في ميكانيكيا الطائرات خاصة في الجناح واسطح السيطرة. نموذج جناح مع قلاب خلفي بثلاث درجات حرية تم تمثيله عدديا و نظريا. تم استخدام برنامج FLUENT لغرض حساب الخواص الايروديناميكية بالاضافة الى استخدام صيغة دوهامل لتمثيل الاحمال الايروديناميكية نظريا. تم تحديد الاستجابة الديناميكية لنظام جناح-قلاب من خلال استخدام الماتلاب (MATLAB) و التكامل بطريقة Runge-Kutta وتم مقارنة النتائج مع تجارب عملية سابقة. بينت النتائج ان الاحمال الايروديناميكية والاستجابة الديناميكية للجناح-قلاب تزداد بزيادة سرعة التدفق ومن ناحية اخرى فان استجابة المائع-هيكل تؤدي الى حالة محدد من التذبذب الدوري المستمر عندما تكون سرعة التدفق مساوية او اكثر من سرعة الرفرفة.

الكلمات الرئيسية: هيكل - مائع, الجناح, اسطح السيطرة, ايروداينمك .

1. INTRODUCTION

Aeroelasticity can be defined as the science which studies the mutual interaction between aerodynamic, elastic of structure and inertial forces. The analysis of dynamic characteristics of either complex or simple structures is quite developed nowadays as far as numerical and experimental methods are concerned. Hence, it is correct to state that reliability in aeroelastic calculations is strongly dependent on the correct evaluation of the aerodynamic operator, **Marques** and **Azevedo, 2007**.

Flutter is one of the most representative topics of aeroelasticity. Flutter is a complex phenomenon where structural modes are simultaneously coupled and excited by aerodynamic loads. In a more formal way, flutter is the condition where an aircraft component exhibits a self-sustained oscillatory behaviour at speeds higher than the critical one, **Wright, 1991**. With recent advances in CPU speeds, current research has turned toward the application of computational • fluid dynamics (CFD) models to the solution of these aeroelastic problems. By the use of an unsteady Euler or Navier–Stokes CFD algorithm coupled with a structural dynamics solver, the complete aeroelastic response of the structure can be predicted. However, the major limitation in applying such a CFD solution is the computational time required to run a full aeroelastic simulation due to the high dimensionality of even the simplest geometry, **Cowan et al, 2001.**

A three degree-of-freedom aeroelastic airfoil section with control surface free play were modeled theoretically as a system of piecewise linear state-space models. They were investigated by **Conner et al., 1997and Liu et al., 2001.** The wing flutter calculated by integrated computational fluid dynamics (CFD) and computational structural dynamics (CSD) method. The coupled CFD–CSD method simulates the aeroelastic system directly on the time domain to determine the stability of the aeroelastic system. Computational fluid dynamics (CFD) solver technique for modeling unsteady aerodynamic forces used in time-domain aeroelastic analysis. The system identification as was predicted by **Cowan et al., 2001. Tricky, 2002.** It could accurately model the unsteady aerodynamic forces for complex aerospace structures of practical interest**. They** presented the effects of a free play structural nonlinearity on an aeroelastic in the three-degree-of-freedom airfoil model. **Dowell et al., 2003** analyzed the effective of leading and trialing edges control surfaces on the airfoil. He used a simple control strategy, then used a combination of leading-and trailing-edge control surface rotations to maintain lift and roll effectiveness and to minimize control surface rotations. **Le Maître et al., 2003,** investigated numerically the aeroelastic flutter derivative of a two-dimensional airfoil by means of Navier–Stokes simulation solver employed influence matrix techniques to determine the exact boundary conditions and a conformal mapping of the physical space. **Ardelean et al., 2006,** designed a new piezoelectric actuator which meets the requirements for trailing edge flap actuation in both stroke and force to study the aeroelastic control of wings with trailing-edge control surfaces. Wind tunnel experiments showed that air flow has a little influence on flap deflection, suggesting good actuation authority. **Marqui et al., 2006,** investigated the flutter parameters for two-degree-of-freedom flexible mounting rigid wings tests with in wind tunnel. The plunging and pitching flutter obtained with this experimental system was described as the combination of structural bending and torsion vibration modes. **Marques and Azevedo, 2007,** used the unsteady computational fluid dynamics tool to calculate the aerodynamic operator for aeroelastic analysis of lifting surfaces in the transonic regime. The flow problem was modeled by the two-dimensional Euler equations using the finite volume method applied in an unstructured grid context. The state-dependent Riccati equation method was derived for aeroelastic response and flutter suppression with control surface free play and Theodorsen theory for aerodynamics of

airfoil section with trialing edge flap were studies by **Li et al., 2010. Ghommem et al., 2012**, studied the response of aeroelastic system consisting of a plunging and pitching rigid airfoil, supported by nonlinear translational and torsional springs, used a three-dimensional code based on the unsteady vortex lattice method to predict the unsteady aerodynamic loads for coupled model of the wing flow interaction. **Vasconcellos et al., 2012,** used a different representations (discontinuous, polynomial and hyperbolic tangent) for control surface freeplay nonlinearity in a three degree of freedom aeroelastic system. **Abdelkefi et al., 2013,** investigated analytically and experimentally the dynamics of an aeroelastic system consisting of two degrees of freedom airfoil section supported by a linear spring in the plunge degree of freedom and a nonlinear spring in the pitch degree of freedom and as well the aerodynamic loads was represented by the quasi-steady and an unsteady formulations. **Saxena** and **Agrawal, 2013** used FLUENT software to study the flow separation over airfoil at different angle of attacks. **Kim** and **Chang, 2014,** studied the effect of a low Reynolds number on the aerodynamic characteristics of a pitching NACA0012 airfoil. The result showed that the phase angle, at which boundary-layer events occurred, was in an inverse proportion to the increase in Reynolds number.

The goals of the present work can be summarized as follow**:**

(a)- A CFD tool is applied with structured two-dimensional meshes around airfoil with control surface to obtain the aerodynamic characteristics at different freestream speed, angles of attack and flap angles.

(b) Predict the flutter speed of the three degrees-of-freedom airfoil section with trialing edge flap.

(c) Investigate the aeroelastic response of plunging, pitching and flap pitching for the airfoil with control surface at freestream speed under, equal and above flutter speeds. The aerodynamic loads are approximated using the Duhamel formulation.

The validity of flutter speed prediction and aeroelastic response are determined through comparison with the experiments of **Conner et al., 1997.** Good agreement was determined.

2. COMPUTATIONAL FLUID DYNAMICS (CFD)

Computational fluid dynamics is a subject that has played an extremely important role in recent studies of aerodynamics. The possibility of numerically treating a broad range of phenomena which occur in flows over bodies of practically any geometry has numerous advantages over experimental determinations, such as greater flexibility together with time and financial resource savings. However, obtaining more reliable numerical results for a growing number of situations has been one of the major recent challenges in many science fields **Marques** and **Azevedo, 2007.** The simulation of the flow was carried out by running ANSYS FLUENT software which based on the solution of the Navier-Stokes equations using the finite-volume method under the same value of the response of airfoil for Angle Of Attack (AOA) and flap pitching angles.

The grid generator ANSYS FLUENT CFD is used to mesh the domain. **Fig.1** presents the airfoil element domain. To increase the grid points at the surface of the wall, skewed mesh should be avoided.

3. AEROELASTIC MODEL

The aeroelastic system modeled of three degrees-of-freedom, two dimension NACA 0012 wing section, constrained to move with degrees of freedom, namely the plunge (h), pitch (α), and control surface angle (β) motions, as shown in **Fig. 2.** The elastic axis is located at distance *ab*

from the mid chord. The mass center of wing section is located at distance $x_\alpha b$ from the elastic axis. Both distances are positive when measured towards the airfoil flap. The cb and $x_\beta b$ distances are the distance from the hinge line of the flap and distance from the mass center of the flap to the mid chord respectively.

The non-dimensional aeroelastic equation of motion for the airfoil with trailing edge control surface are given by **Li et al., 2010.**

$$r_\alpha^2\ddot{\alpha} + \left[r_\beta^2 + (c-a)x_\beta\right]\ddot{\beta} + x_\alpha\ddot{h} + r_\alpha^2\omega_\alpha^2 F(\alpha) = \frac{M_\alpha}{(mb^2)} \qquad (1-a)$$

$$\left[r_\beta^2 + (c-a)x_\beta\right]\ddot{\alpha} + r_\beta^2\ddot{\beta} + x_\beta\ddot{h} + r_\beta^2\omega_\beta^2 G(\beta) = \frac{M_\beta}{(mb^2)} \qquad (1-b)$$

$$x_\alpha\ddot{\alpha} + x_\beta\ddot{\beta} + \left(\frac{m_t}{m}\right)\ddot{h} + \omega_h^2 h = \frac{L}{(mb)} \qquad (1-c)$$

Where

$$x_\alpha = \frac{S_\alpha}{m_w b}, \qquad x_\beta = \frac{S_\beta}{m_w b}, \qquad r_\alpha^2 = \frac{I_\alpha}{m_w b^2}, \qquad r_\beta^2 = \frac{I_\beta}{m_w b^2}$$

The matrix of structural damping is created in this model according to **Conner et al., 1997**, the natural frequency $\omega_i = \sqrt{\lambda_i}$, where λ_i is eigenvalue and the eigenvector matrix are obtained from the left-hand side structure components of equations (1-a, 1-b and 1-c). Then the system modal mass matrix $\boldsymbol{M_{mod}} = \boldsymbol{\Lambda^T M_s \Lambda}$ and the modal damping matrix $\boldsymbol{B_{mod}}$ can be calculated as

$$\mathbf{B_{mod}} = \begin{bmatrix} 2m_\alpha\omega_\alpha\varsigma_\alpha & 0 & 0 \\ 0 & 2m_\beta\omega_\beta\varsigma_\beta & 0 \\ 0 & 0 & 2m_h\omega_h\varsigma_h \end{bmatrix} \qquad (2)$$

Where $m_\alpha, m_\beta \; and \; m_h$ are the values at the diagonal entries of $\boldsymbol{M_{mod}}$ and $\varsigma_\alpha, \varsigma_\beta \; and \; \varsigma_h$ are the measured damping ratios. The structure damping matrix can be determined as $\boldsymbol{B_s = (\Lambda^T)^{-1} B_{mod} (\Lambda)^{-1}}$.

The Theodorsen approach is used to model the unsteady aerodynamic force and moments $L, M_\alpha \; and \; M_\beta$ in incompressible flow were calculated and written as by Theodorsen, 1935**.**

$$\begin{aligned} M_\alpha = & -\rho b^2 \{ \pi (1/(2-a)) U b\dot{\alpha} + \pi b^2 (1/(8+a^2))\ddot{\alpha} + (T_4 + T_{10})U^2\beta + (T_1 - T_8 - \\ & (c-a)T_4 + (1/2)T_{11})Ub\dot{\beta} - [T_7 + (c-a)T_1]b^2\ddot{\beta} - a\pi b\ddot{h}\} + \\ & 2\rho U b^2 \pi((a+1)/2)C(k)\left(U\alpha + \dot{h} + b(1/(2-a))\dot{\alpha} + 1/\pi T_{10} U\beta + b(1/2\pi)\, T_{11}\dot{\beta}\right) \end{aligned} \qquad (3)$$

$$M_\beta = -\rho b^2\{(-2T_9 - T_1 + T_4((a-1)/2))Ub\dot{\alpha} + 2T_{13}b^2\ddot{\alpha} + (1/\pi)U^2\beta(T_5 - T_4T_{10}) - ((1/2\pi))Ub\dot{\beta}T_4T_{11} - (1/\pi)T_3b^2\ddot{\beta} - T_1b\ddot{h}\} \times \rho Ub^2T_{12}C(k)(U\alpha + \dot{h} + b(1/(2-a)\dot{\alpha} + 1/\pi T_{10}U\beta + b((1/2\pi))T_{11}\dot{\beta}) \quad (4)$$

$$L = -\rho b^2(U\pi\dot{\alpha} + \pi\ddot{h} - \pi ba\ddot{\alpha} - UT_4\dot{\beta} - T_1b\ddot{\beta}) - 2\pi\rho UbC(k)(U\alpha + \dot{h} + b(1/(2-a))\dot{\alpha} + 1/\pi T_{10}U\beta + b(1/2\pi)T_{11}\dot{\beta}) \quad (5)$$

Where the T functions are given in Appendix A

The aerodynamic force and moment in Eqs. (3)-(5) are dependent on reduced frequency *k*. so Eqs. (1-a) - (1-c) are restricted to simple harmonic oscillation. Aerodynamics in Eq. (3)–(5) is dependent on Theodorsen's function, *C(k),* where *k* is the non-dimensional reduced frequency of harmonic oscillation. So the aerodynamics is restricted to simple harmonic motion. In order to simulate arbitrary motion of the airfoil, the loading associated with Theodorsen's function *C(k)f(t)* is replaced by the Duhamel formulation in the time domain and written as, **Li et al., 2010.**

$$L_c = C(k)f(t) = f(0)\emptyset(\tau) + \int_0^\tau \frac{\partial f(\sigma)}{\partial\sigma}\phi(\tau - \sigma)d\sigma \quad (6)$$

Where

$$f(t) = U\alpha + \dot{h} + b\left(\frac{1}{2-a}\right)\dot{\alpha} + 1/\pi T_{10}U\,\beta + b\left(\frac{1}{2\pi}\right)T_{11}\dot{\beta} \quad (7)$$

and $\phi(\tau)$ is Wagner function. In this work, convenient approximation of Sears is used as

$$\phi(\tau) \approx c_0 - c_1e^{-c_2\tau} - c_3e^{-c_4\tau} \quad (8)$$

the coefficient in equation (8) are $c_1 = 0.165,\ c_2 = 0.0455,\ c_3 = 0.335\ and\ c_4 = 0.3$. in order to simplify the Theodorsen function, rewrite the Duhamel integral using integration by parts ,

$$L_c = f(\tau)\phi(0) + \int_0^\tau f(\sigma)\frac{\partial\phi(\tau-\sigma)}{\partial\sigma}\,d\sigma \quad (9)$$

And following the state space method proposed by **Li et al., 2010**.

$$L_c = (c_0 - c_1 - c_3)f(t) + c_2c_4(c_1 + c_3)\bar{x} + (c_1c_2 + c_3c_4)\dot{\bar{x}} \quad (10)$$

With the introduction of two augmented variables $x_{a1} = \bar{x},\ x_{a2} = \dot{\bar{x}}$, Eq. (1) can be product as

$$(\mathbf{M_s} - \mathbf{M_{NC}})\ddot{\mathbf{x}} + \left(\mathbf{B_s} - \mathbf{B_{NC}} - \frac{\mathbf{1}}{\mathbf{2RS_2}}\right)\dot{\mathbf{x}} + \left(\mathbf{K_s} - \mathbf{K_{NC}} - \frac{\mathbf{1}}{\mathbf{2RS_1}}\right)\mathbf{x} - \mathbf{RS_3x_a} = \mathbf{0} \quad (11)$$

Where $x = [\alpha \quad \beta \quad h/b]^T$ and $x_a = [x_{a1} \quad x_{a2}]^T$.
In the state space form, this equation is written as

$$\dot{\mathbf{X}} = \mathbf{A}(\mathbf{X})\mathbf{X} \tag{12}$$

The solution Algorithm and definition of the matrices in Eqs. (11) and (12) are presented in Appendix B.

4. RESULTS AND DISCUSSIONS

4.1 Aerodynamic Results

Once the meshes are generated, the next step will be simulations. There were more than 70 cases run in ANSYS/Fluent which different AOA from -6 to 6 degree with step 2 degrees as well as the same pitch angle differential with all AOA step and different freestream velocities. These simulations yielded solutions to the two dimensional flow fields around the airfoil with trailing edge flap.

The lift and drag forces at (4) degrees angle of attack (α) as well as various flap pitching angles (β) are analyzed with increasing velocity and it is cleared that lift force increases when velocity is increased as well decreasing of flap pitching angle as shown in **Fig. 3- a and Fig. 3- b. These figures** show that the drag forces were affected slightly with values of (β) while they increased with increasing the velocity. Pitching moments are greatly influenced with (β) as well increased with velocity as shown in **Fig. 3-c** which showed when ($\beta = 2^{\circ}$) that the pitching moment was increased but decreased when velocity more than 15 m/s.

The simulations were run with limit of responses of varying angles of attack from (-6 to +6 degree step 2) and flap angles from (-6 to +6 degree step 2) at velocity equals to (25 m/s) for the analytical calculated flutter. The AOA and flap angle variation play important role in the lift generation as well as the effect of drag and pitching moments. For maximization of the lift in the aircraft wings, the trialing edge flap angle should be down, while the AOA must be increasing as verified in **Fig. 4-which** shows increasing of lift force with decreasing the flap angle (down) while AOA increased. **Fig. 4-b** shows that the increasing of drag force was happened when the AOA was increased-decreased. Flap angles as well as the result observed that the increment of drag force with swing of airfoil more than variation of flap angle, nevertheless the behavior of the ratio of lift-drag asymptotic to lift force demeanor as shown in **Fig. 4-c**. Finally **Fig. 4-d** illustrates the effect of AOA and flap angle changing to the pitching moment. They were important factors were affecting to airfoil swing result, and that shows that the flap angle was significantly affected to the pitching moment.

Pressure contours at different velocities variations are shown in **Fig. 5**. It can be seen that the pressure increased when the freestream velocity increased with values of 5 to 30 step 5 m/s at zero flap angle and 4 degree AOA. At the same time, pressure contours around the airfoil also was varied. For maximization of the lift in the aircraft wings, the pressure should be low at the upper surface of the wings and high at the bottom surface of the wing. **Fig. 6** shows the pressure distribution around the airfoils at zero flap angle, calculated flutter velocity and swing AOA up/down were zero value. Results show that the pressure on the lower surface of the airfoil is high and the pressure over the upper surface is low only at positive AOA and vice versa which produces inverse lift generation.

Fig. 7 clarifies the dynamic pressure contour at flutter velocity, zero AOA and swing flap angle which affect to the pressure contour even at zero AOA and symmetric airfoil. The velocity distribution around airfoil was affected by the swing of AOA and flap angle. **Fig. 8** displays the velocity contour at swing of AOA and flap angle. It is clear that the maximum velocity was 31 m/s when AOA and flap angles at the same sign i.e. all up or down because it is a case of symmetry. On the other hand when the angles reverse, the maximum velocity was 34 m/s and this is asymmetry case.

4.2 Aeroelastic Response Results

The prediction of flutter speed was obtained by using the results of Eq.(11) where the flutter speed is the value of speed corresponding to the speed at zero real part of one or more eigenvalues which determined to be 25 m/s and compared with **Conner et al 1997** which was (20.6 m/s experimentally and 23.9 m/s analytically).The parameters used in the mathematical models were taken from **Conner et al 1997** and listed as follows: a = -0.5, b = 0.127 m, c = 0.5, s = 0.52 m, $m_T = 1.2895\ kg$, $I_\alpha = 0.01347\ kgm^2, I_\beta = 0.0003264 kgm^2, x_\alpha = 0.434, x_\beta = 0.01996, k_h = 2818.8\ N/m, S_\alpha = 0.08587\ kg\ m, S_\beta = 0.00395\ kg\ m, \rho = 1.225\ kg/m^3, \varsigma_1 = 0.01626, \varsigma_2 = 0.0115\ and\ \varsigma_3 = 0.0113$. The variations of the real parts with wind speed are shown in **Fig 9. Fig. 10** shows the comparison between present work and experimental **Conner et al 1997** for the response of pitch angle at wind speed 6.75 m/s.

Using MATLAB with fourth order Runge-Kutta method has been used for numerical integration with a time step of (0.001) to solve the state-space Eq. (12). Time histories of plunge response were shown in **Fig. 11.** The response determined with wind speed under, equal and above flutter speed. The limit cycle oscillation of plunge amplitude is similar to harmonic motion with speed under and equal flutter speed as well with above flutter speed but the peak value was irregulars peak value with the complete cycle. This may be due to the relatively high unstable values of the plunge displacement.

Pitch angle response converges with time at velocity 20 m/s which less than flutter speed as shown in **Fig. 12** which also shows the limit cycle oscillation continue at the same peak value (4 degree) and this happens at flutter velocity because the damping is zero at this speed where the value of pitching angle reached to (7.4 degree) at 30 m/s wind speed.

Fig. 13 presents the response of flap pitching angle at degree with time at velocity 20 m/s, 25 m/s and 30 m/s it can be noted that the time histories was increased in the peak value and limit cycle oscillation to be irregulars at wind speed above flutter speed value. The rates versus displacement of plunge, pitching and flap pitching are shown in **Figs. 14, 15 and 16** respectively at calculated flutter speed. It can be shown that the behavior and values are symmetry about stable zone which zero value as that the harmonically response which Theodorsen assumptions.

5. CONCLUSION

The objective of this study is to investigate the aeroelastic modeling and flutter analysis of a three degrees-of-freedom airfoil section with trialing edge flap. The steady CFD solution was used to present the aerodynamic characteristics with different freestream speeds, AOA and flap angle, which showed that affect on the aerodynamic forces and moment especially flap angle factor as shown from the pressure distribution and velocity distribution diagrams. Using a standard state-space approximation to Theodorsen aerodynamics for two-dimensional incompressible flow to the fourth order Runge-Kutta numerical integration of a piecewise linear

system to predict the aeroelastic response and flutter behavior which verified with previous experimental work. For experimental test of wing flutter response at velocity over flutter speed was difficult because the risk of model shattering, theoretical investigation discuss the limit cycle oscillation which irregulars response behavior at over flutter speed. The study compared this irregular response with harmonically time histories which obtained at velocity under and equal flutter speeds.

REFERENCES.

- Abdelkefi, A., Vasconcellos, R., Nayfeh, A. H. and Hajj, M. R., 2013, *An analytical and Experimental Investigation into Limit-Cycle Oscillations of An Aeroelastic System*, Nonlinear Dynamics Journal, Vol. 71, PP.159–173.

- Ardelean, E. V., Mark A. M., Cole, D. G and Clark, R. L. 2006 *Active Flutter Control with V-Stack Piezoelectric Flap Actuator* Journal of Aircraft Vol. 43, No. 2 PP. 482-486.

- Balaguru, I., Sendhilkumar, S. 20013 *Numerical and Experimental Investigation on Aerodynamic Characteristics of SMA Actuated Smart Wing Model* International Journal of Engineering and Technology (IJET) Vol. 5, No. 5, PP. 3813-3818.

- Bohbot, J., Garnier, J., Toumit, S. and Darracq, D. 2001 *Computation of the Flutter Boundary of an Airfoil with a Parallel Navier-Stokes Solver,* American Institute of Aeronautics and Astronautics 39th Aerospace Sciences Meeting & Exhibit (AIAA 2001-0572).

- Conner, M. D., Tang, D. M., Dowell, E. H and Virgin, L. N., 1997, *Nonlinear Behavior of A Typical Airfoil Section with Control Surface Freeplay :* A Numerical and Experimental Study, Journal of Fluids and Structures Vol. 11 , PP. 89 – 109.

- Cowan, T. J, Arena, A. S., Jr. and Gupta, K. K 2001, *Accelerating Computational Fluid Dynamics Based Aeroelastic Predictions Using System Identification*, Journal of Aircraft Vol. 38, No. 1, PP. 81-87.

- Dong-HaKima, and Jo-WonChang, 2014, *Low-Reynolds-number Effect on the Aerodynamic Characteristics of a Pitching NACA0012 Airfoil*, Aerospace Science and Technology Vol. 32, PP. 162–168.

- Dowell, E. H., Bliss, D. B. and Clark, R. L 2003, *Aeroelastic Wing with Leading- and Trailing-Edge Control Surfaces*, Journal of Aircraft Vol. 40, No. 3, PP. 559-565.

- Edwards , J . W ., Ashley , H . & Breakwell , J . V . 1979, *Unsteady Aerodynamic Modeling For Arbitrary Motions* . *AIAA Journal* **17 ,** 365 – 374 .

- Fazelzadeh, S. A. and Kalantari, H. A. 2009, *Bending-Torsional Flutter of Wings with an Attached Mass Subjected to a Follower Force*, Journal of Sound and Vibration Vol. 323 PP. 148–162.

- Ghommema, M., Abdelkefi, A., Nuhait,A. O. and .Hajj, M. R. 2012, *Aeroelastic Analysis and Nonlinear Dynamics of an Elastically Mounted Wing*, Journal of Sound and Vibration Vol. 331, PP. 5774–5787.

- Le Maître, O. P., Scanlan, R. H. and Knio, O. M., 2003, *Estimation of the Flutter Derivatives of an NACA Airfoil by Means of Navier–Stokes Simulation*, Journal of Fluids and Structures, Vol. 17, PP. 1-28.

- Li, D., Guo, S., and Xiang, J. 2010, *Aeroelastic Dynamic Response and Control of an Airfoil Section with Control Surface Nonlinearities*, Journal of Sound and Vibration Vol. 329, PP. 4756–4771.

- Liu, F., Cai, J., Zhu, Y., Tsai, H. M. and Wong, A. S 2001 *Calculation of Wing Flutter by a Coupled Fluid-Structure Method*, Journal of Aircraft Vol. 38, No. 2, PP 334-342.

- Marques, A. N and Azevedo, J. L 2007, *Application of CFD-Based Unsteady Forces for Efficient Aeroelastic Stability Analyses*, Journal of Aircraft Vol. 44, No. 5, PP. 1499-1512.

- Marqui, C. D., Rebolho, C. D., Belo E. D. and Marques F. D, 2006, *Identification of Flutter Parameters for a Wing Model*, J. of the Braz. Soc. of Mech. Sci. & Eng Vol. XXVIII, No. 3, PP. 339-346.

- McNamara, J. J. and Friedmann, P. P. 2007, *Flutter-Boundary Identification for Time-Domain Computational Aeroelasticity*, AIAA Journal Vol. 45, No. 7, PP. 1546-1555.

- Parker, G. H., Maple, R. C., and Beran, P. S., 2007, *Computational Aeroelastic Analysis of Store-Induced Limit-Cycle Oscillation*, Journal of Aircraft Vol. 44, No. 1 PP. 48-59.

- Platanitis, G., and Strganac,T. W., 2004, *Control of a Nonlinear Wing Section Using Leading- and Trailing-Edge Surfaces*, Journal of Guidance, Control, and Dynamics Vol. 27, No. 1, PP. 52-58.

- PrabhakaraRao, P. and Sampath.V., 2014, *CFD Analysis on Airfoil at High Angles of Attack*, International Journal of Engineering Research Vol. 3, No.7, PP. 430-434.

- Rajakumar, S., Ravindran., D., 2010, *Computational Fluid Dynamics of Wind turbine Blade at Various Angles of Attack and Low Reynolds Number*, International Journal of Engineering Science and Technology Vol. 2, No 11, PP. 6474-6484.

- Saxena, G. and Agrawal, M., 2013, *Aerodynamic Analysis of NACA 4412 Airfoil Using CFD*, International Journal of Emerging Trends in Engineering and Development Vol.4, No. 4, PP. 416-423.

- Srivastava, R and Reddy, T. S. 1997 *Forced Response Analysis Using a Two-Dimensional Multistage Euler Aeroelastic Solver*, Journal of Aircraft Vol. 34, No. 1, PP. 114-119.

- Theodorsen, T., 1935, *General Theory of Aerodynamic Instability and The Mechanism of Flutter*, NACA Report 496.

- Trickeyl, S. T., Virgina, N. and Dowell, E. 2002, *The Stability of Limit-Cycle Oscillations in a Nonlinear Aeroelastic System* ,Proceedings: Mathematical, Physical and Engineering Sciences, Vol. 458, No. 2025. PP. 2203-2226.

- Vasconcellos, R., Abdelkefi, A, Marques, F. D and Hajj, M. R. 2012, *Representation and Analysis of Control Surface Freeplay Nonlinearity*, Journal of Fluids and Structures Vol. 31, PP. 79–91.

- Woodgate, M. A., Badcock, K. J., Rampurawala, A. M., Richards, B. E. and Nardini, D. 2005, *Aeroelastic Calculations for the Hawk Aircraft Using the Euler Equations*, Journal of Aircraft Vol. 42, No. 4,PP. 1005-1012.

- Wright, J.R., 1991, "*Introduction to Flutter of Winged Aircraft*", von Karman Institute for Fluid Dynamics, Lecture series 01: Elementary Flutter Analysis.

NOMENCLATURE

AOA	angle of attack, degree
a	non-dimensional distance from airfoil mid-chord to elastic axis
b	airfoil semi-chord
Pa	Pascal, N/m^2
s	wing span, m
C(k)	generalized Theodorsen function
CPU	central processor unit
c	non-dimensional distance from airfoil mid-chord to the control surface hinge line
c_i	coefficients of Wagner's function
h	plunge displacement, m
k	reduced frequency
L	aerodynamic lift
M_α, M_β	aerodynamic moment of wing-aileron and of aileron
m	mass of wing-aileron (per unit span), kg/m
m_t	total mass of wing-aileron and support blocks (per unit span), kg/m
r_α	radius of gyration of wing-aileron
r_β	reduced radius of gyration of aileron
t	time, sec
U	free stream velocity, m/s
$\boldsymbol{X}_a$	vector of augmented variables
x_α	non-dimensional distance from airfoil elastic axis to center of mass

x_β non-dimensional distance from aileron hinge line to center of mass
α pitch angle about the elastic axis, degree
β aileron displacement about the hinge line, degree
ρ density of air, kg/m^3
ς damping ratio
τ time delay
ω uncoupled natural frequency, rad/s

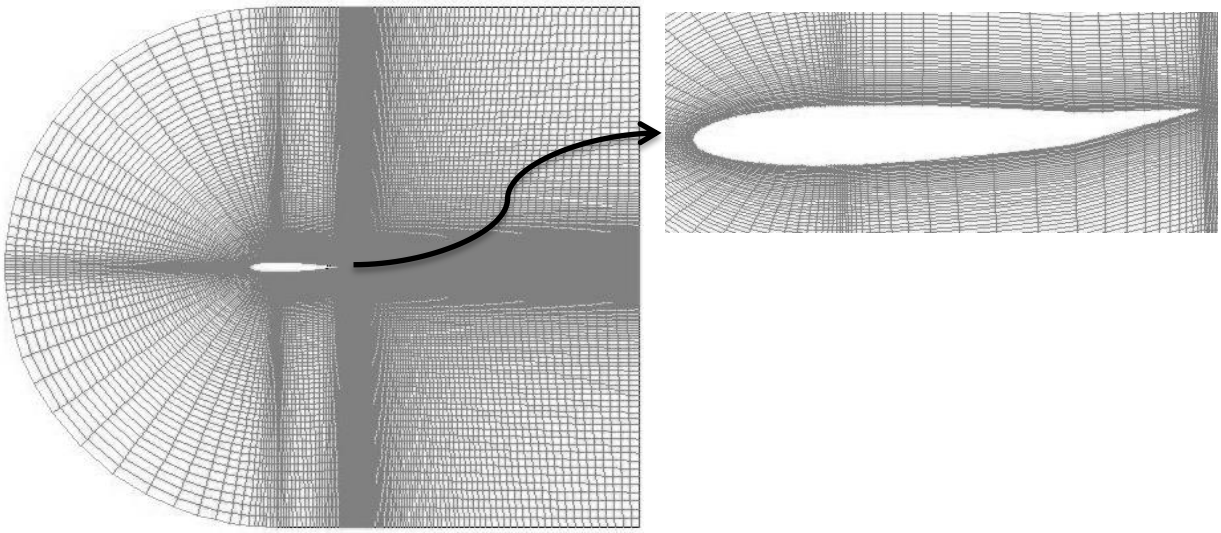

Figure1. Airfoil domain mesh.

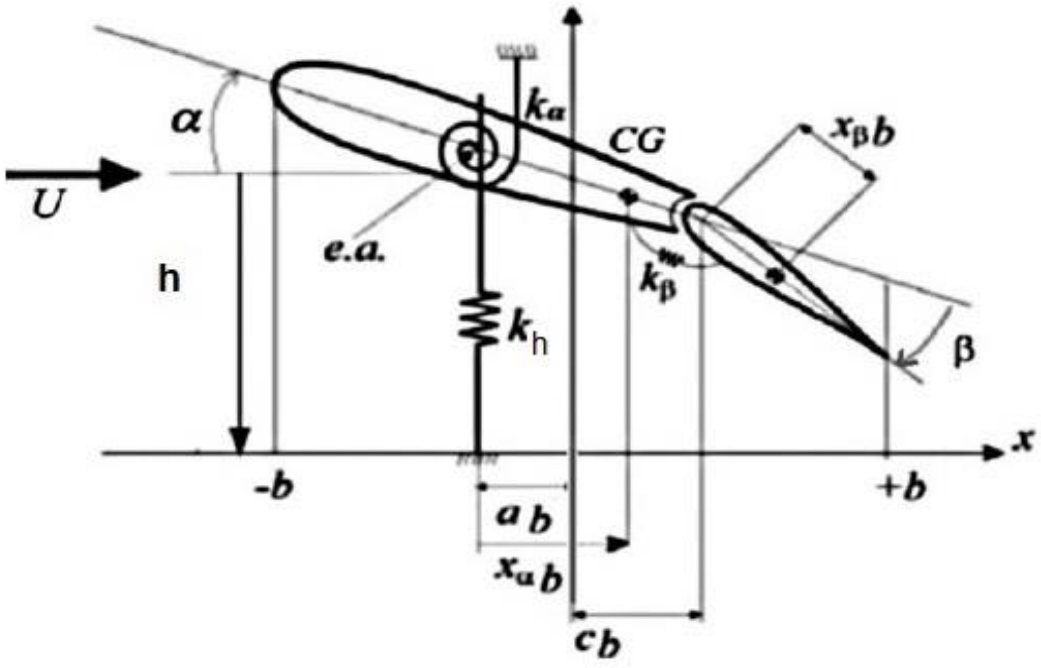

Figure 2. Schematic of airfoil section with trialing edge flap.

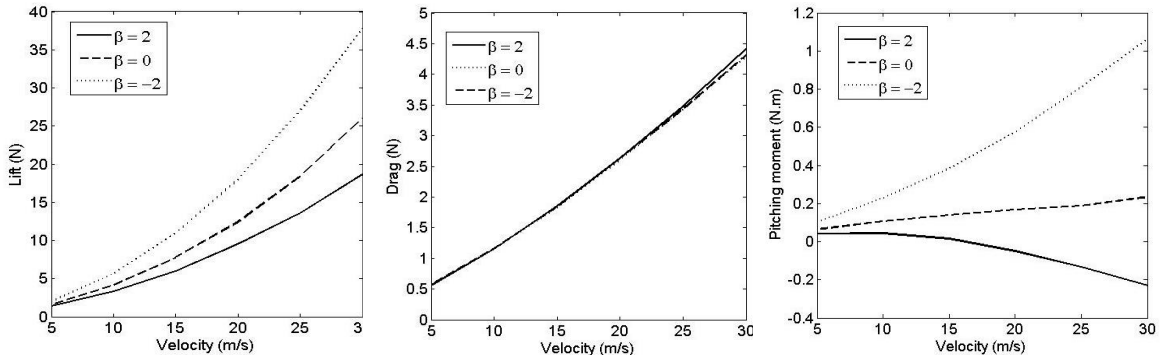

(a) (b) (c)

Figure 3. Variations of (a) the lift forces, (b) the drag forces and (c) the pitching moment as function of freestream velocity for various flap pitching angle (β).

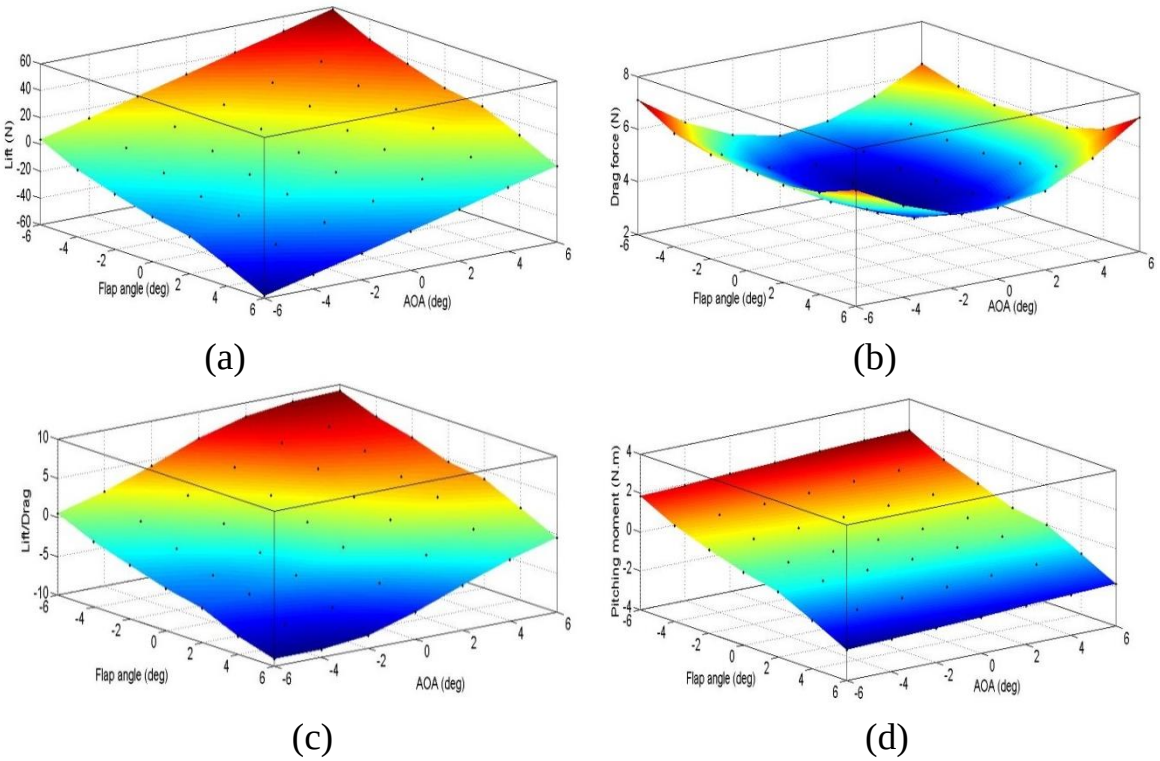

(a) (b)

(c) (d)

Figure 4. Effect of increasing –decreasing of angle of attack and flap angle to the (a) lift force (b) drag force (c) lift/drag ratio and (d) pitching moment.

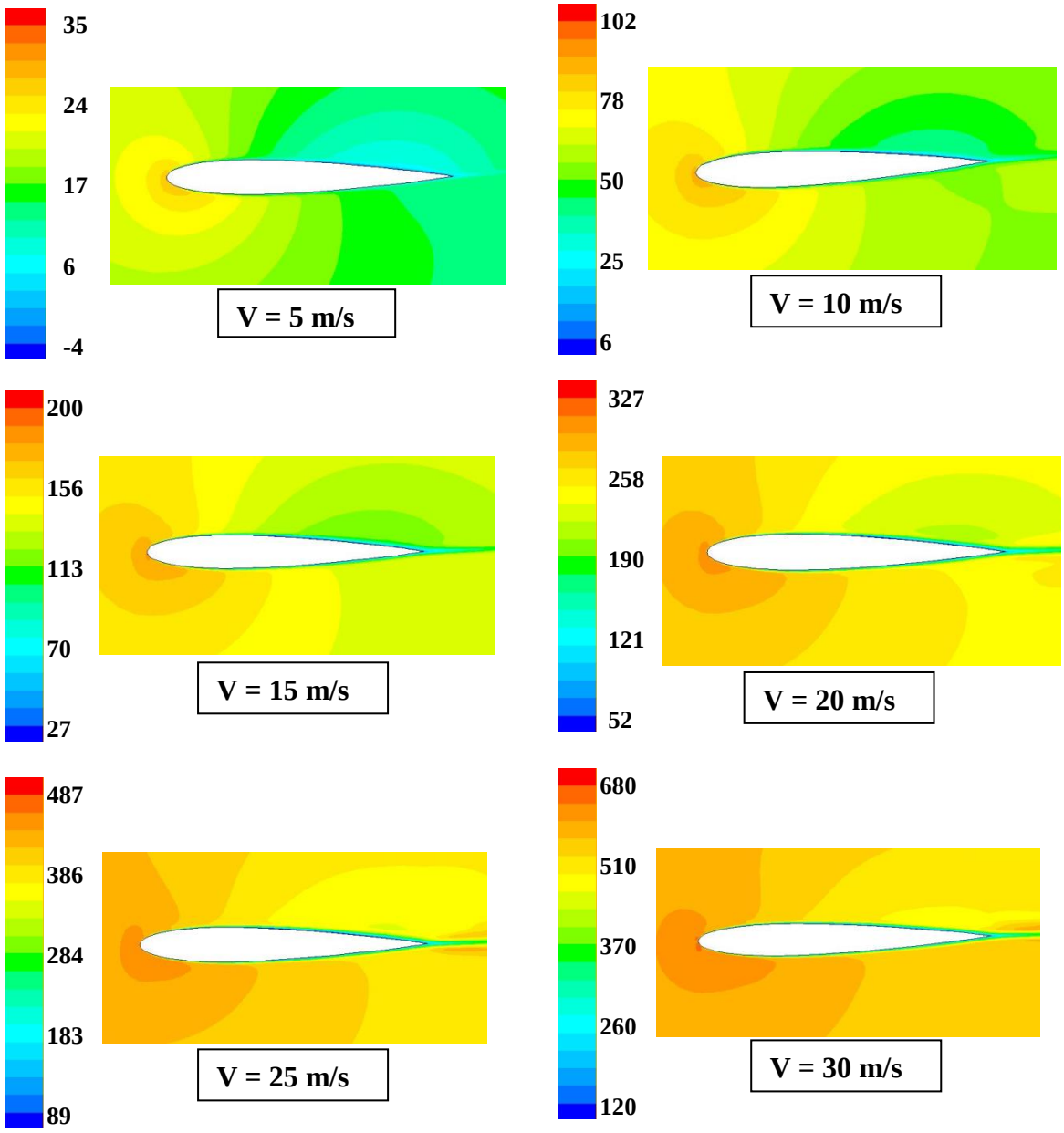

Figure 5. Contours of total pressure (Pa) around the airfoil at different free stream velocity, zero flap angle and 4 degree AOA.

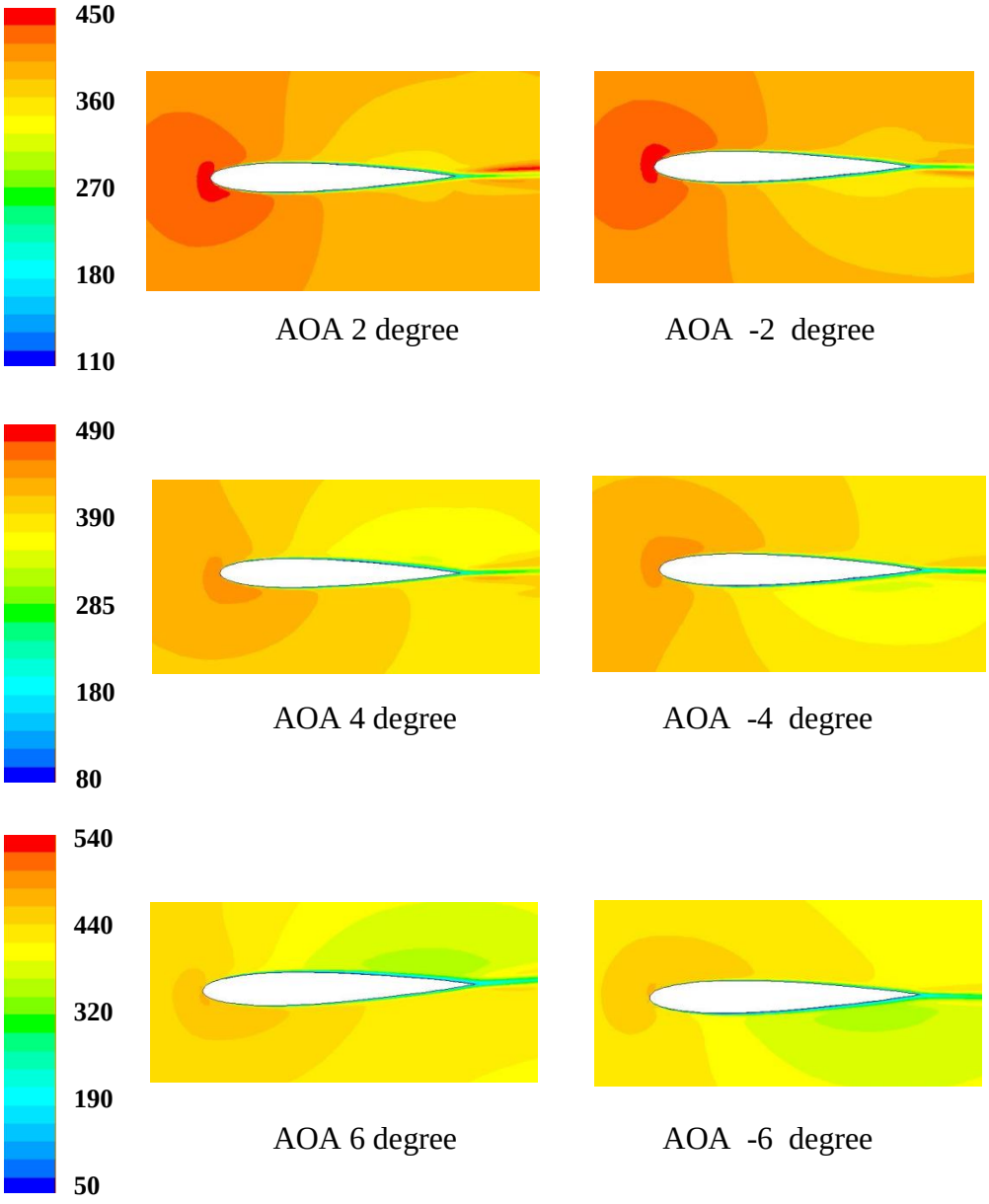

Figure 6. Contours of total pressure (Pa) around the airfoil at different AOA, zero flap angle and 25 m/s air speed.

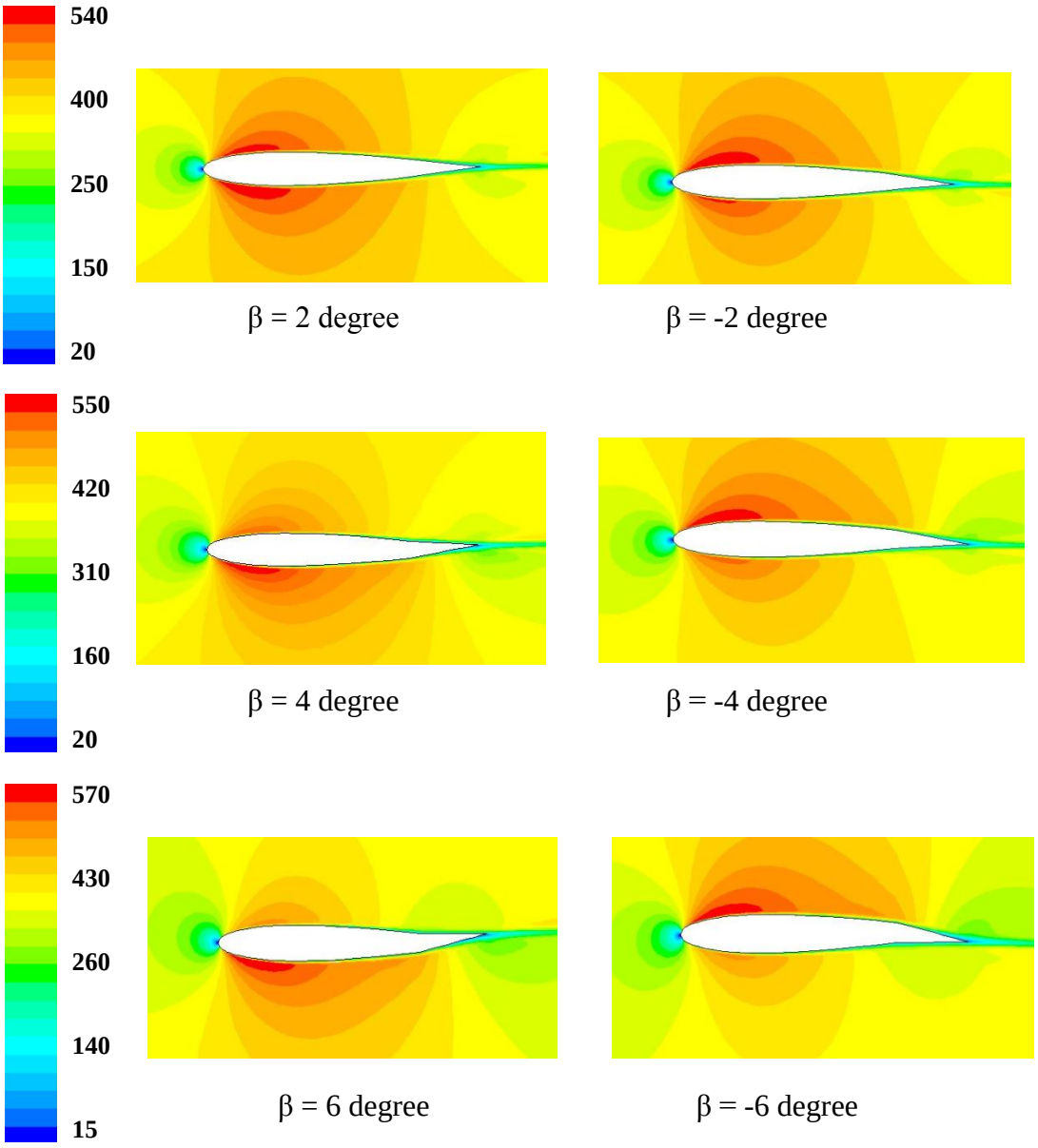

Figure 7. Dynamic pressure (Pa) around the airfoil at different flap angle, zero AOA and 25 m/s air speed.

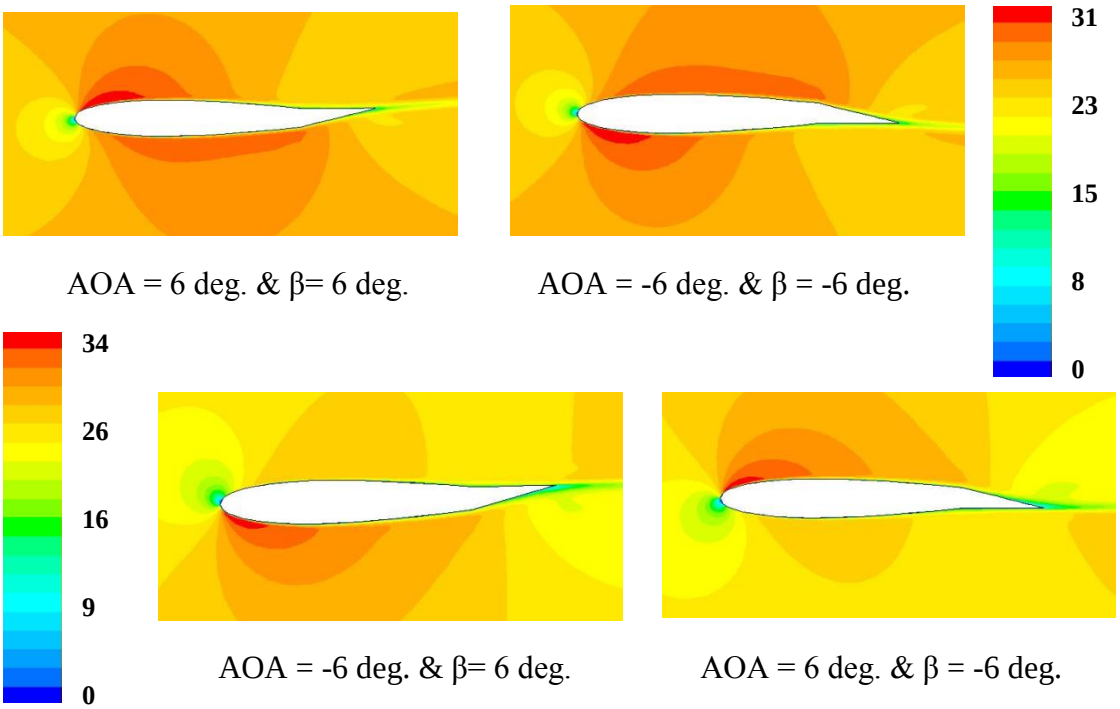

Figure 8. Velocity (m/s) distribution around the airfoil at fluttering profile for V=25.

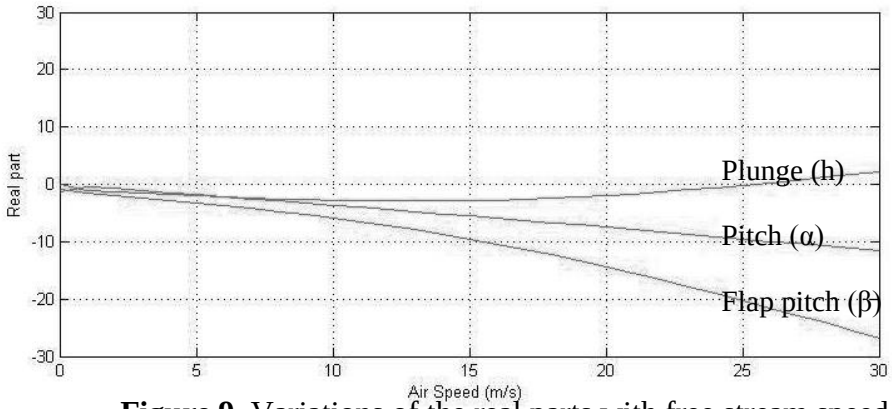

Figure 9. Variations of the real parts with free stream speed.

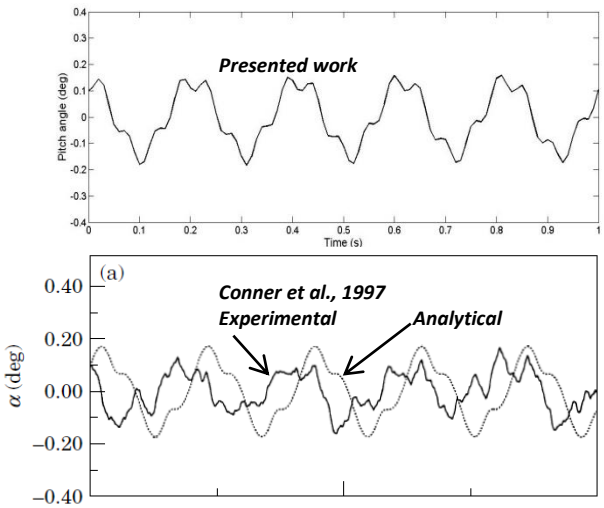

Figure 10. Pitch time histories for the low frequency limit-cycle at $U = 0.27\ U_f$.

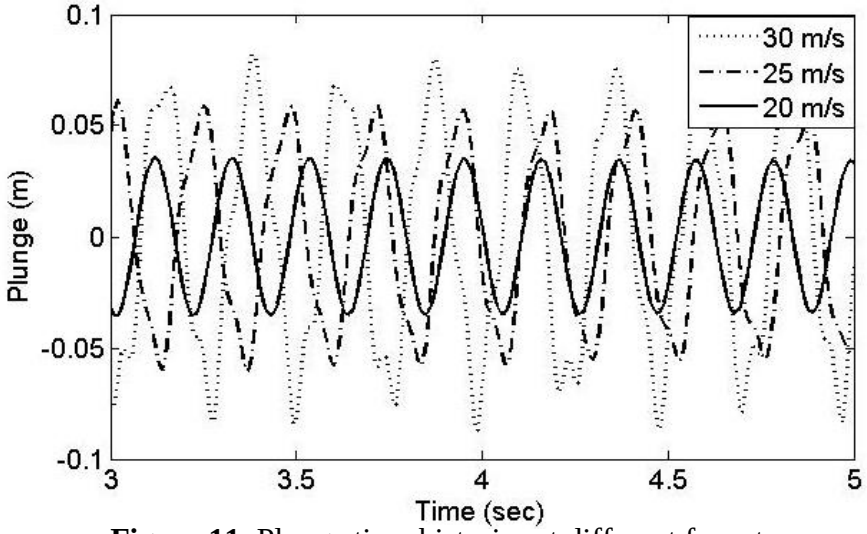

Figure 11. Plunge time histories at different free stream.

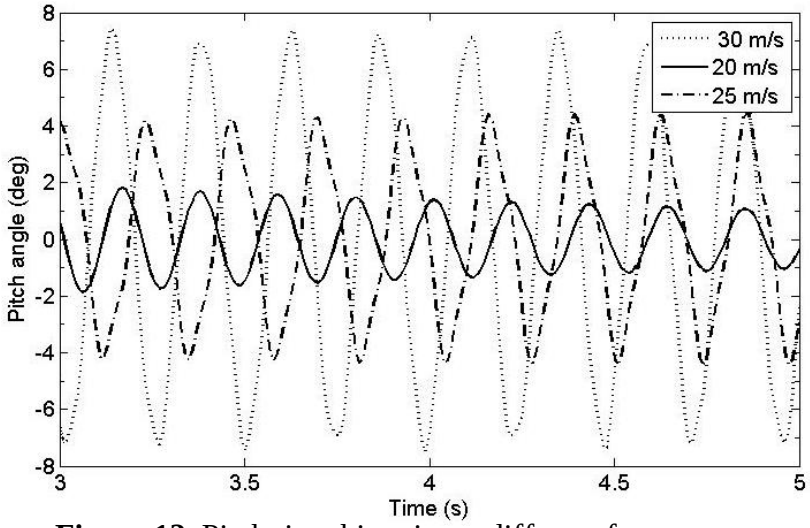

Figure 12. Pitch time histories at different free stream.

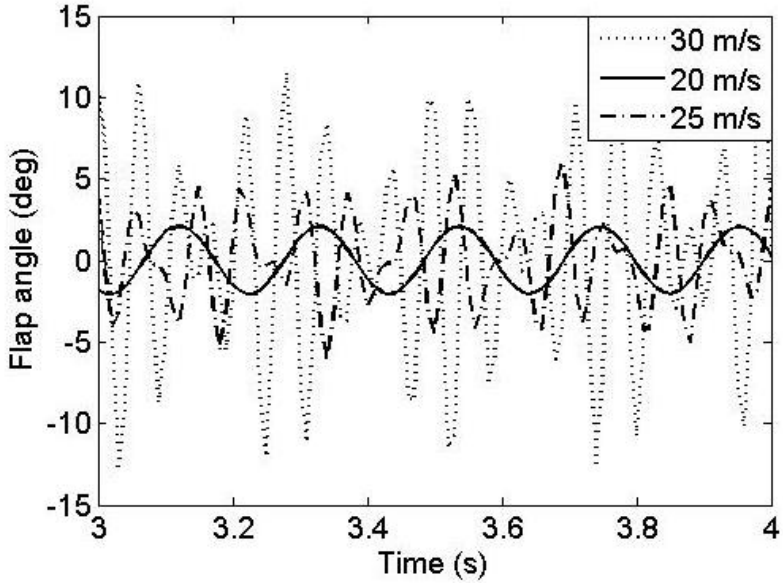

Figure 13. Flap pitch time histories at different free stream.

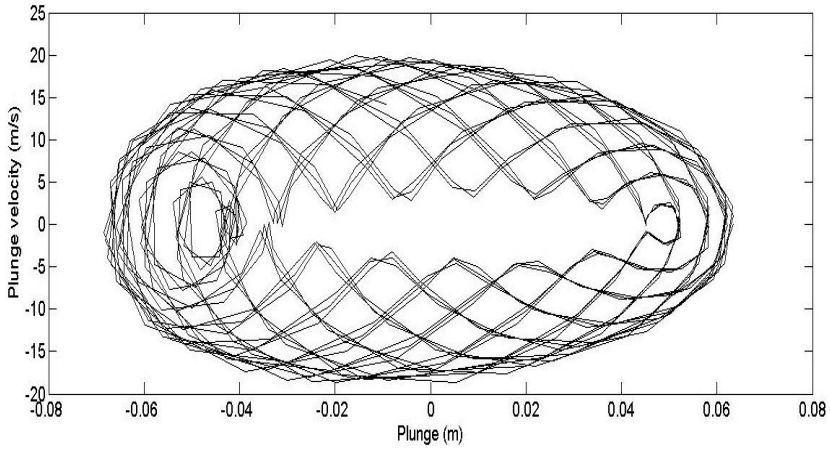

Figure 14. Phase portraits of plunge at flutter speed.

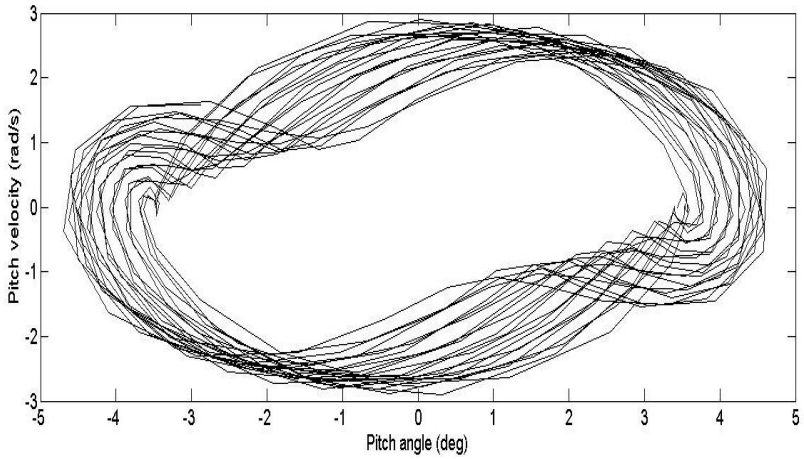

Figure 15. Phase portraits of pitch at flutter speed.

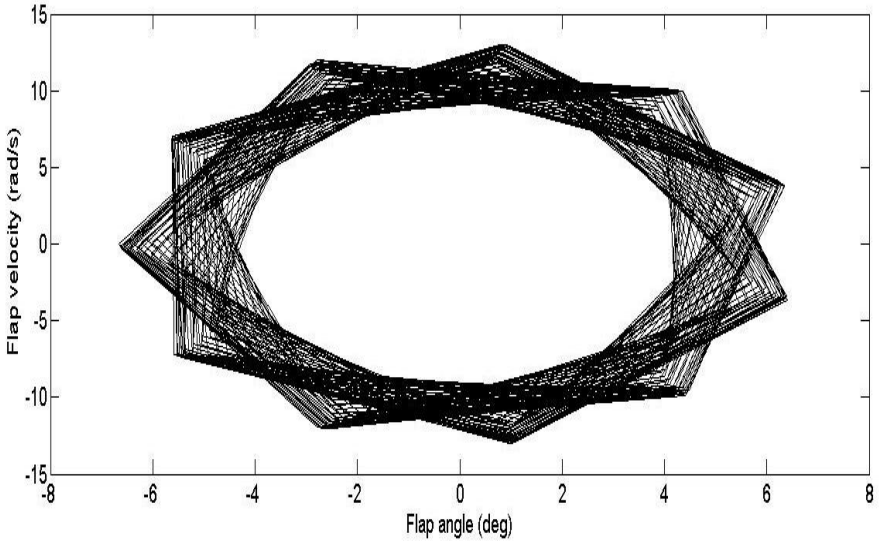

Figure 16. Phase portraits of flap pitch at flutter speed.

APPENDIX A. Theodorsen Constant in Eqs. (3)-(5)

$$T_1 = -\frac{1}{3}\sqrt{1-c^2}(2+c^2) + \cos^{-1} c$$

$$T_3 = -\left(\frac{1}{8}\right)c(1-c^2)(5c^2+4) + \frac{1}{4}(7+2c^2)\sqrt{1-c^2}\cos^{-1} c - \left(\frac{1}{8}+c^2\right)(\cos^{-1} c)^2$$

$$T_4 = c\sqrt{1-c^2} - \cos^{-1} c$$

$$T_5 = -(1-c^2) + 2c\sqrt{1-c^2}\cos^{-1} c - (\cos^{-1} c)^2$$

$$T_7 = \left(\frac{1}{8}\right)c(7+2c^2) - \left(\frac{1}{8}+c^2\right)\cos^{-1} c$$

$$T_8 = -\left(\frac{1}{3}\right)(1+2c^2)\sqrt{1-c^2} + c\cos^{-1} c$$

$$T_9 = \frac{1}{2}\left[\frac{1}{3}\left(\sqrt{1-c^2}\right)^3 + aT_4\right]$$

$$T_{10} = \sqrt{1-c^2} + \cos^{-1} c$$

$$T_{11} = (\cos^{-1} c)(1-2c) + \sqrt{1-c^2}(2-c)$$

$$T_{12} = \sqrt{1-c^2}(2+c) - (\cos^{-1} c)(2c+1)$$

$$T_{13} = \frac{1}{2}[-T_7 - (c-a)T_1]$$

APPENDIX B. Definitions of Matrices in Eqs. (11)-(12)

$$\mathbf{M}_s = \begin{bmatrix} r_\alpha^2 & r_\beta^2 + (c-a)x_\beta & x_\beta \\ r_\beta^2 + (c-a)x_\beta & r_\beta^2 & x_\beta \\ x_\alpha & x_\beta & M_t/M \end{bmatrix}$$

$$\mathbf{B}_t = (\boldsymbol{\Lambda}^{\boldsymbol{T}})^{-1}\begin{bmatrix} 2m_\alpha\omega_\alpha\varsigma_\alpha & 0 & 0 \\ 0 & 2m_\beta\omega_\beta\varsigma_\beta & 0 \\ 0 & 0 & 2m_h\omega_h\varsigma_h \end{bmatrix}\boldsymbol{\Lambda}^{-1}$$

$$\mathbf{K}_s = \begin{bmatrix} r_\alpha^2\omega_\alpha^2 & 0 & 0 \\ 0 & r_\beta^2\omega_\beta^2 & 0 \\ 0 & 0 & \omega_h^2 \end{bmatrix}$$

$$\mathbf{M}_{\mathrm{NC}} = -\frac{\rho}{m}\begin{bmatrix} \pi b^2\left(\frac{1}{8}+a^2\right) & -(T_7+(c-a)T_1)b^2 & -\pi a b^2 \\ 2T_{13}b^2 & -T_3 b^2/\pi & -T_1 b^2 \\ -\pi a b^2 & -T_1 b^2 & \pi b^2 \end{bmatrix}$$

$$\mathbf{B}_{\mathrm{NC}} = -\frac{\rho}{m}\begin{bmatrix} \pi\left(\frac{1}{2}-a\right)Ub & (T_1 - T_8 - (c-a)T_4 + T_{11}/2)Ub & 0 \\ \left(-2T_9 - T_1 + T_4\left(a-\frac{1}{2}\right)\right)Ub & -T_4 T_{11} Ub/(2\pi) & 0 \\ \pi Ub & -UT_4 b & 0 \end{bmatrix}$$

$$\mathbf{K}_{\mathrm{NC}} = -\frac{\rho}{m}\begin{bmatrix} 0 & (T_4+T_{10})U^2 & 0 \\ 0 & (T_5 - T_4 T_{10})U^2/\pi & 0 \\ 0 & 0 & 0 \end{bmatrix}$$

$$\mathbf{R} = [2\pi\rho U\left(a+\frac{1}{2}\right)/m \quad -\rho U T_{12}/m \quad -2\pi\rho U/m]^T$$

$$\mathbf{S}_1 = [U \quad T_{10}U/\pi \quad 0]$$

$$\mathbf{S}_2 = \left[b\left(\frac{1}{2}-a\right) \quad bT_{11}/2\pi \quad b\right]$$

$$\mathbf{S}_3 = [c_2 c_4 (c_1+c_3)U^2/b \quad (c_1 c_2 + c_3 c_4)U]$$

$$\mathbf{A} = \begin{bmatrix} 0 & \mathbf{I}_{3\times 3} & 0 \\ -\mathbf{M}_t^{-1}\mathbf{K}_t & -\mathbf{M}_t^{-1}\mathbf{B}_t & \mathbf{M}_t^{-1}\mathbf{D} \\ \mathbf{E}_1 & \mathbf{E}_2 & \mathbf{F} \end{bmatrix}$$

$$\mathbf{M}_{\mathrm{t}} = \mathbf{M}_{\mathrm{s}} - \mathbf{M}_{\mathrm{NC}},$$

$$\mathbf{B}_{\mathrm{t}} = \mathbf{B}_{\mathrm{s}} - \mathbf{B}_{\mathrm{NC}} - 1/2\mathbf{R}\mathbf{S}_2,$$

$$\mathbf{K}_{\mathrm{t}} = \mathbf{K}_{\mathrm{s}} - \mathbf{K}_{\mathrm{NC}} - 1/2\mathbf{R}\mathbf{S}_1, \quad \mathbf{D} = \mathbf{R}\mathbf{S}_3$$

$$\mathbf{E}_1 = \begin{bmatrix} 0 & 0 & 0 \\ U/b & UT_{10}/(\pi b) & 0 \end{bmatrix},$$

$$\mathbf{E}_2 = \begin{bmatrix} 0 & 0 & 0 \\ (1/2-a) & T_{11}/(2\pi) & 1 \end{bmatrix},$$

$$\mathbf{F} = \begin{bmatrix} 0 & 1 \\ -c_2 c_4 U^2/b & -(c_2+c_4)U/b \end{bmatrix}$$

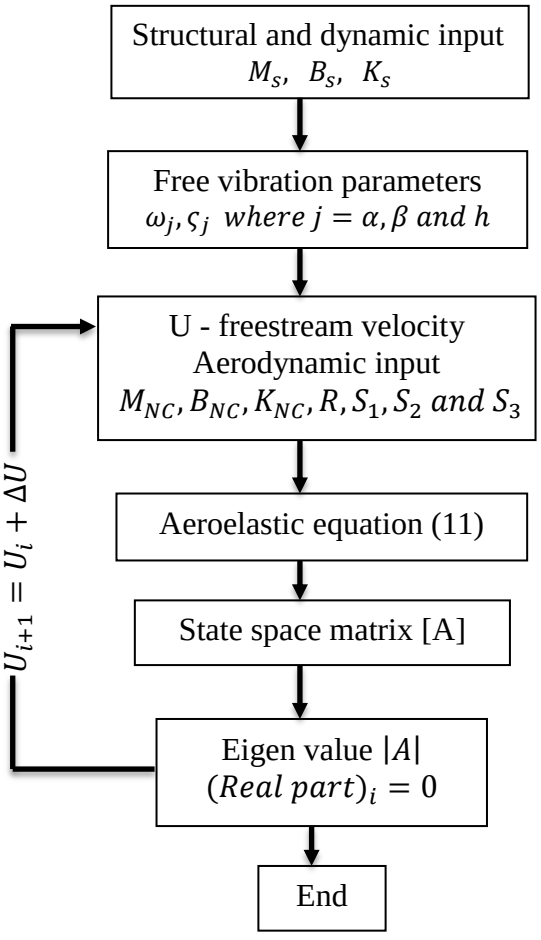

Solution Algorithm to find flutter speed